DOI: 10.1002/ejic.200900709

Tetranuclear Copper(II) Complexes Bearing Cu_4O_6 and Cu_4O_4 Cores: Synthesis, Structure, Magnetic Properties, and DFT Study

Atanu Banerjee,[a] Reena Singh,[a] Pallab Mondal,[a] Enrique Colacio,[b] and Kajal Krishna Rajak*[a]

Keywords: Tetranuclear complexes / Magnetic properties / Density functional calculations / Copper

The reaction of $Cu(ClO_4)_2 \cdot 6H_2O$ with N_4O_3 coordinating heptadentate (H_3L^1) and N_2O coordinating tridentate reduced Schiff base (HL^2) ligands yielded copper(II) tetranuclear complexes $[Cu_4(L^1)_2](ClO_4)_2$ (**1**) and $[Cu_4(L^2)_4](ClO_4)_4$ (**2**), respectively. Complex **1** crystallizes in the cubic system, space group $Fd\bar{3}c$, with unit-cell parameters $a = b = c = 43.124(5)$ Å, $Z = 48$, whereas complex **2** crystallizes in the space group $P4_12_12$ in the tetragonal crystal system with $Z = 8$ and unit-cell parameters $a = b = 17.113(4)$ Å, $c = 44.150(4)$ Å. The X-ray structures of **1** and **2** have revealed a Cu_4O_6 core in **1** and a Cu_4O_4 core in **2**. Complexes **1** and **2** show intramolecular antiferromagnetic interaction with moderate $|J|$ values (104.2 cm^{-1} for **1** and 155.1 cm^{-1} for **2**). The moderate $|J|$ value can be explained by the existence of only one bridging alkoxido group between each pair of copper(II) atoms and the out-of-plane displacement of the alkoxido carbon atom from the Cu–O–Cu plane. Broken-symmetry density functional theory (BSDFT) has been used to justify the exchange pathways.

Introduction

The chemistry of multinuclear metal complexes has aroused abiding interest in recent years because of their relevance to the multimetal active sites of various metalloproteins.[1,2] The incorporation of metallic centers that have an unpaired spin in the compounds, and hence the isolation of a polymeric metal complex, is also a burgeoning field of inorganic and material research due to their widespread application in the area of molecular-based magnetic devices.[3–11] In this connection, our interest lies in the design, isolation, and characterization of polynuclear copper(II) complexes using polydentate ligands.

In this paper we will explore the synthesis of tetranuclear copper(II) complexes using suitable conformationally labile ligands that may act simultaneously as bridging and terminal ligands to the metal ions. The present work is associated with the symmetrical N_4O_3 coordinating heptadentate and N_2O coordinating tridentate reduced Schiff base ligands and their complexation with Cu^{II} ions.

The chelation of the heptadentate ligand ensures the formation of a stable μ-phenoxido- and μ-alkoxido-bridged tetranuclear copper(II) complex, and an alkoxide-bridged tetranuclear copper(II) complex has been obtained with a chiral N_2O coordinating ligand. The complexes have been characterized by IR, UV/Vis, and electron paramagnetic resonance (EPR) spectroscopic techniques. X-ray structures and the variable-temperature magnetic moment of the complexes have been determined. Their electrochemical behavior is also examined.

Tetranuclear complexes that have Cu_4O_6 and Cu_4O_4 cores offer easy access to the model system ($3d^9$, $3d^9$, $3d^9$, $3d^9$), which gives us the opportunity to understand the behavior of the unpaired electrons and hence their magnetic properties.[12–20] Thus, here we also present a full broken-symmetry density functional theory (BSDFT) investigation to obtain better insight into the exchange coupling of these systems.

Results and Discussion

Synthesis and Characterization

One N_4O_3 coordinating heptadentate ligand (H_3L^1) and one N_2O coordinating ligand (HL^2) derived from an L-amino alcohol have been utilized in the present work. The stoichiometric reaction of $Cu(ClO_4)_2 \cdot 6H_2O$ with the N_4O_3 coordinating heptadentate ligand (H_3L^1) in the presence of triethylamine gives a μ-phenoxido- and μ-alkoxido-bridged tetranuclear complex of formula $[Cu_4(L^1)_2](ClO_4)_2$ (**1**). When the same reaction was carried out with HL^2, it furnished an alkoxido-bridged tetranuclear copper(II) species, $[Cu_4(L^2)_4](ClO_4)_4$ (**2**).

[a] Inorganic Chemistry Section, Department of Chemistry, Jadavpur University,
Kolkata 700032, India
E-mail: kajalrajak@hotmail.com
kkrajak@chemistry.jdvu.ac.in
[b] Departamento de Química Inorgánica, Facultad de Ciencias, Universidad de Granada,
18071 Granada, Spain

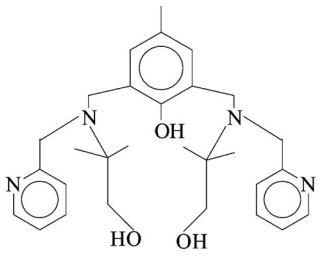

H_3L^1

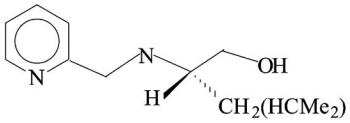

HL^2

The C–$O_{alkoxido}$ vibrations occur at 1051 and 1024 cm^{-1} for **1** and **2**, respectively.[21] The ClO_4^- stretches for **1** and **2** appear at 623, 1091 and 625, 1093 cm^{-1}, respectively. The N–H stretches for complex **2** occur at 3447 cm^{-1}.

The UV/Vis spectra of solutions of the complexes in acetonitrile (CH_3CN) were recorded and display two well-resolved peaks along with a shoulder. A characteristic copper d–d transition is observed at 747 and 656 nm for **1** and **2**, respectively. The band in the region 250–320 nm can be attributed to the ligand absorption band and alkoxido- and/or phenoxido-to-copper ligand-to-metal charge-transfer (LMCT) excitation.[22,23]

The complexes are electroactive in acetonitrile [potentials referenced vs. a saturated calomel electrode (SCE)]. The complexes exhibit two irreversible waves at 0.95, –0.76 V for **1** and 1.35, –0.82 V for **2**. The anodic peak potential is assigned to $Cu^{II} \rightarrow Cu^{III}$ oxidation, whereas that of the cathodic one is due to $Cu^{II} \rightarrow Cu^{I}$ reduction.

The X-band EPR spectra of the complexes were recorded at 77 K for polycrystalline samples in frozen solution (DMF/toluene). The complexes show no triplet spectra in solution, which is indicative of the EPR-silent nature of the complexes. However, a weak signal is observed, which is probably due to the presence of a small amount of noncoupled species.[24]

The minor mol fraction of the noncoupled species (ρ) is 0.9% for **1**, which has a $g_{\|}$ value of about 2.22 and a $g_{\perp}$ of about 2.06, whereas for **2** we have found that $g_{\|} = 2.18$ and $g_{\perp} = 2.04$ ($\rho = 0.3\%$).

Crystal Structure

The crystal structures of the complexes have been determined. A view of the cationic part of the tetranuclear entity of complexes **1** and **2** is shown in Figure 1a and Figure 2a, respectively. Selected interatomic distances and angles are listed in Tables 1 and 2.

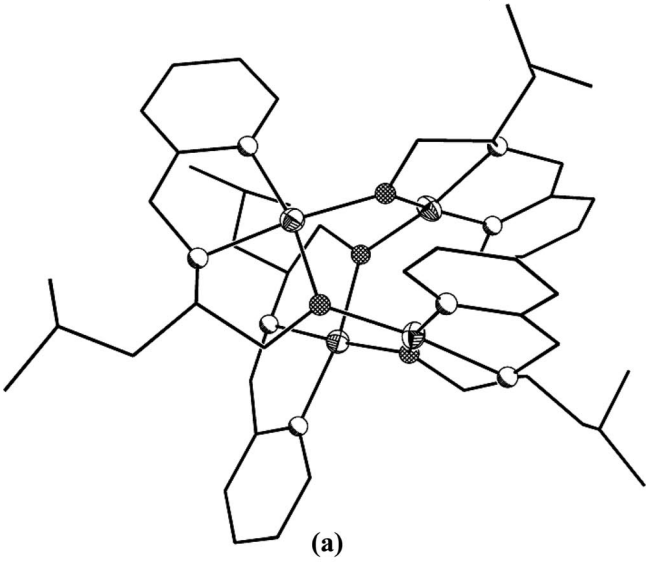

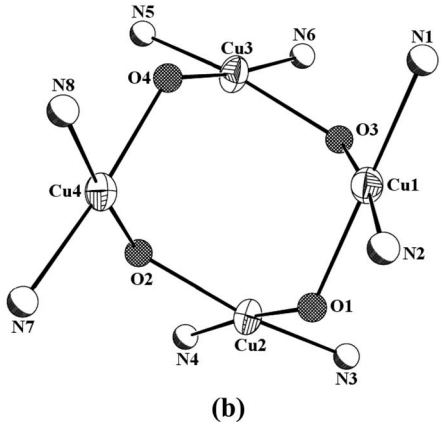

Figure 1. (a) Structure of the cationic part of $[Cu_4(L^1)_2](ClO_4)_2$. (b) View of the $Cu_4N_8O_6$ core.

$[Cu_4(L^1)_2](ClO_4)_2$ (1)

In **1**, the copper atom is bonded through alkoxido (O1,O1A,O1B,O1C) and phenoxido (O2,O2A) groups, thus forming a mixed-bridged tetranuclear copper species (Figure 1b). It is to be noted that in the lattice each copper center is connected with the other three adjacent copper centers by means of one phenoxido and two alkoxido bridges; the Cu···Cu distance is 3.579(7) Å. The geometry around the copper atom is a distorted square pyramid (τ = 0.06).[25] In the slightly distorted square-pyramid geometry, the equatorial positions are occupied by two nitrogen atoms (N1 and N2) and two alkoxido-bridged oxygen atoms (O1 and O1A), whereas the axial position is occupied by a bridging phenoxide atom (O2). The Cu–N and Cu–$O_{alkoxido}$ bond lengths are in the range of 2.03–2.09 Å and 1.93–1.97 Å, respectively. The axial Cu–$O_{phenoxido}$ bond length is 2.056(2) Å.

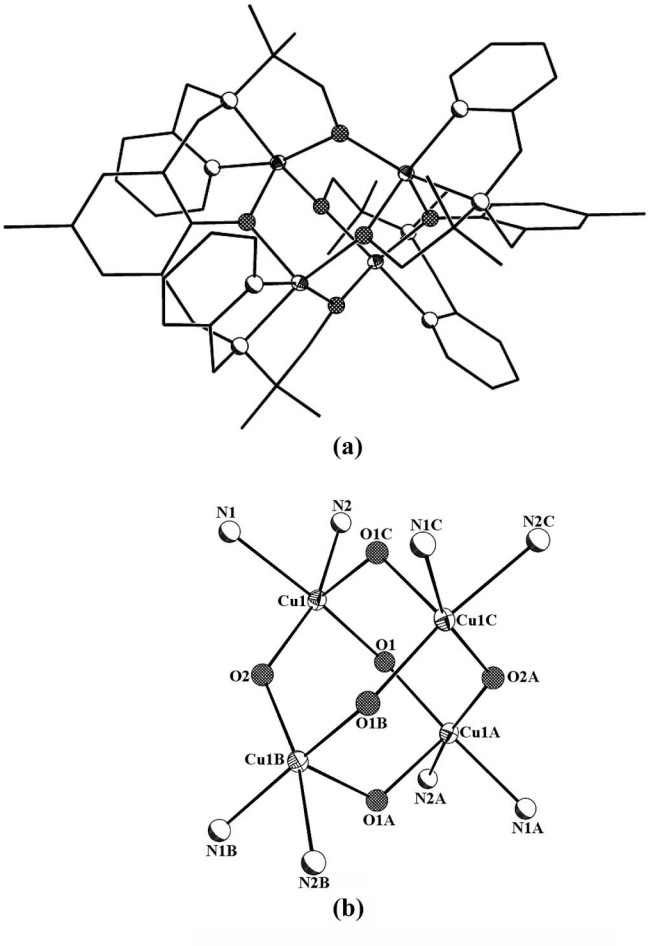

Figure 2. (a) Structure of the cationic part of $[Cu_4(L^2)_4](ClO_4)_4$. (b) View of the $Cu_4N_8O_4$ core.

Table 1. Selected distances [Å] and angles [°] for complex **1**.

Distances			
Cu1–N1	2.096(4)	Cu1–O1A	1.969(3)
Cu1–N2	2.039(4)	Cu1–O2	2.056(2)
Cu1–O1	1.975(3)	Cu···Cu	3.580(4)
Angles			
N1–Cu1–N2	81.43(16)	O1–Cu1–N2	163.18(15)
N1–Cu1–O1A	166.83(15)	O2–Cu1–O1A	101.80(12)
N2–Cu1–O1A	93.07(16)	O2–Cu1–N1	90.37(14)
O1–Cu1–O1A	97.47(11)	O2–Cu1–N2	91.71(15)
O1–Cu1–O2	98.88(12)	Cu1–O1–Cu1A	130.11(16)
O1–Cu1–N1	85.45(15)	Cu1–O2–Cu1B	121.0(2)

$[Cu_4(L^2)_4](ClO_4)_4$ (2)

The tetranuclear entity **2** crystallizes in the tetragonal space group $P4_12_12$, in which the four copper ions are bridged through the alkoxido oxygen atom of the ligand, thus forming a cyclic Cu_4O_4 core (Figure 2b). In the complex, each copper coordination sphere CuO_2N_2 has a distorted square-planar geometry. The Cu–O and Cu–N bond lengths are not unusual. The Cu···Cu separation falls in the range 3.40–3.65 Å.

Table 2. Selected distances [Å] and angles [°] for complex **2**.

Distances			
O1–Cu1	1.867(7)	N1–Cu1	1.946(5)
O1–Cu2	1.908(6)	N2–Cu1	1.998(8)
O2–Cu2	1.934(7)	N3–Cu2	1.940(5)
O2–Cu4	1.909(7)	N4–Cu2	1.994(8)
O3–Cu1	1.930(6)	N5–Cu3	1.938(5)
O3–Cu3	1.922(6)	N6–Cu3	1.997(8)
O4–Cu3	1.896(6)	N7–Cu4	1.951(5)
O4–Cu4	1.916(7)	N8–Cu4	1.968(8)
Cu1···Cu2	3.325(6)	Cu2···Cu3	3.651(7)
Cu1···Cu3	3.394(8)	Cu2···Cu4	3.450(6)
Cu1···Cu4	3.604(6)	Cu3···Cu4	3.387(6)
Angles			
O1–Cu1–O3	91.3(3)	O3–Cu3–N5	162.2(3)
O1–Cu1–N1	167.9(3)	O3–Cu3–N6	84.1(3)
O1–Cu1–N2	84.3(3)	O4–Cu3–N5	98.5(3)
O1–Cu2–O2	96.1(3)	O4–Cu3–N6	171.9(4)
O1–Cu2–N3	96.8(3)	O4–Cu4–N7	167.9(3)
O1–Cu2–N4	174.0(3)	O4–Cu4–N8	85.2(3)
O2–Cu2–N3	162.8(3)	N1–Cu1–N2	84.1(3)
O2–Cu2–N4	84.2(3)	N3–Cu2–N4	84.2(2)
O2–Cu4–O4	91.2(3)	N5–Cu3–N6	83.6(3)
O2–Cu4–N7	100.8(3)	N7–Cu4–N8	82.8(3)
O2–Cu4–N8	176.2(3)	Cu1–O1–Cu2	121.8(3)
O3–Cu1–N1	99.9(3)	Cu1–O3–Cu3	123.6(3)
O3–Cu1–N2	173.4(3)	Cu2–O2–Cu4	127.7(3)
O3–Cu3–O4	95.5(3)	Cu3–O4–Cu4	125.4(4)

Magnetic Properties

The temperature dependences of χ_M and $\chi_M T$ for complex **1** (χ_M is the molar magnetic susceptibility per Cu_4 unit) in an applied magnetic field of 0.5 T are displayed in Figure 3. The value of $\chi_M T$ at room temperature (1.19 $cm^3 mol^{-1} K$) is significantly lower than that expected for four uncoupled Cu^{II} ions with $g = 2$ (1.5 $cm^3 mol^{-1} K$), which is probably due to the existence of medium to strong antiferromagnetic interactions between the copper(II) ions mediated by the alkoxido and/or phenoxido bridging groups. The $\chi_M T$ product shows a continuous decrease with decreasing temperature to reach a value of 0.05 $cm^3 mol^{-1} K$ at 2 K, thus supporting the presence of antiferromagnetic interactions between the Cu^{II} ions. In keeping with this, the thermal variation of χ_M shows a broad maximum near 70 K. Below this temperature, χ_M decreases to reach a minimum at 25 K and then increases to a value of 0.0025 $cm^3 mol^{-1}$ at 2 K. This low-temperature tail is due to the presence of a small amount of noncoupled species.

Copper(II) atoms in complex **1** adopt a quasitetrahedral arrangement with two different types of bridges (see Scheme 1): (i) alkoxido connecting the pairs Cu1–Cu2, Cu1–Cu3, Cu2–Cu4, and Cu3–Cu4, with a Cu–O–Cu angle of 130.11° and a Cu···Cu distance of 3.576 Å, and (ii) phenoxido connecting Cu1–Cu4 and Cu2–Cu3, with a Cu–O–Cu angle of 121° and a Cu···Cu distance of 3.58 Å. In keeping with this symmetry, the spin Hamiltonian describing the low-lying states in zero fields may be written as shown in Equation (1).

$$H = -J_1(S_1S_2 + S_1S_3 + S_2S_4 + S_3S_4) - J_2(S_1S_4 + S_2S_3) \quad (1)$$

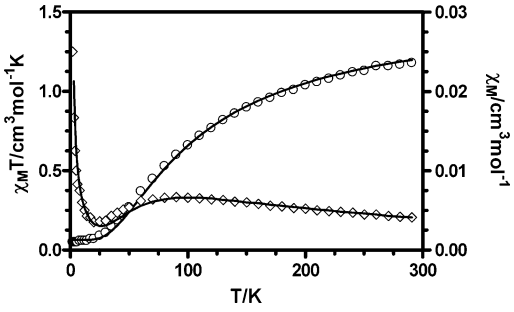

Figure 3. Plots of χ_M (right) and $\chi_M T$ (left) for **1**. The solid line corresponds to the best fit (data fit with starting values from DFT) for $J_1 = -104.2\ cm^{-1}$, $J_2 = -2.2\ cm^{-1}$, $g = 2.01$, and $\rho = 0.9\%$ with a fixed TIP of $240 \times 10^{-6}\ cm^3\,mol^{-1}$ ($R = 3 \times 10^{-4}$).

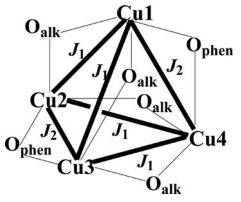

Scheme 1.

It should be noted at this point that alkoxido bridges connect equatorial positions in the square-pyramidal coordination environments of neighboring copper(II) ions (the Addison parameter $\tau = 0.06$ indicates that the geometry is very close to perfect square-pyramidal). The phenoxido bridges, however, link two axial positions on neighboring copper(II) ions, where the density of the unpaired electron is very small (the $d_{x^2-y^2}$ magnetic orbital is directed to the basal donor atoms). Therefore, the magnetic exchange coupling mediated by the phenoxido-bridge magnetic pathway should be very small.[26–28] In view of this, in a first approach, only the J_1 parameter for the alkoxido-bridge pathway was considered. The $\chi_M T$ versus T data were simulated through a full-matrix diagonalization method by using the MAGPACK[29] program with the above Hamiltonian and $J_2 = 0\ cm^{-1}$. A ρ parameter (the molar fraction of the noncoupled species) was included to account for the noncoupled impurity. It was assumed that the noncoupled impurity follows the Curie law and has the same molecular weight and the same g factor as the tetranuclear compound. The best-fit parameters are: $J_1 = -104.3\ cm^{-1}$, $g = 2.01$, and $\rho = 0.9\%$ with a fixed temperature-independent paramagnetism (TIP) of $240 \times 10^{-6}\ cm^3\ mol^{-1}$ ($R = 1 \times 10^{-5}$ {$R = [\Sigma(\chi_{obsd.} - \chi_{calcd.})^2]/\Sigma(\chi_{obsd.})^2$}). The J_1 and J_2 parameters were obtained from DFT calculations (see below). The DFT-calculated values were then used as a starting point to fit the experimental data, thus leading to the following parameters: $J_1 = -104.2\ cm^{-1}$, $J_2 = -2.2\ cm^{-1}$, $g = 2.01$, and $\rho = 0.9\%$ with a fixed TIP of $240 \times 10^{-6}\ cm^3\,mol^{-1}$ ($R = 3 \times 10^{-4}$).

In the case of **2**, the $\chi_M T$ value ($1.22\ cm^3\,mol^{-1}\,K$) at 300 K is also significantly reduced relative to the expected value for four independent $S = ½$ centers with $g = 2$ ($1.5\ cm^3\,mol^{-1}\,K$). Figure 4 represent the χ_M and $\chi_M T$ versus T for complex **2**. The appearance of a maximum in the χ_M versus T plot near 150 K and the decrease in $\chi_M T$ upon cooling suggest strong antiferromagnetic interactions (a Curie tail is present in χ_M below 25 K due to a paramagnetic impurity). In **2**, the four copper atoms also adopt a distorted tetrahedral disposition with Cu···Cu distances in the range 3.325–3.450 Å.

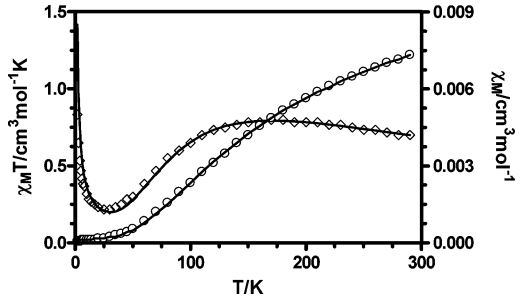

Figure 4. Plot of χ_M (right) and $\chi_M T$ (left) for **2**. The solid line represents the best fit (data fit with starting values from DFT) for $J_4 = -155.1\ cm^{-1}$, $J_3 = -1.0\ cm^{-1}$, $g = 2.174$, and $\rho = 0.3\%$ with a fixed TIP of $240 \times 10^{-6}\ cm^3\,mol^{-1}$ ($R = 2 \times 10^{-4}$).

In the complex, the alkoxido bridges connect the pairs of copper atoms, Cu1–Cu2, Cu1–Cu3, Cu3–Cu4, and Cu4–Cu2 with Cu–O–Cu angles in the range 121.8–125.3° (see Scheme 2). Because the Cu···Cu distances and angles for these pairs are close, all of them were considered to have the same J value. On the other hand, there is not any bridging ligand that links the pairs Cu1–Cu4 and Cu2–Cu3. Therefore, the magnetic coupling between these pairs of copper atoms must be very small.

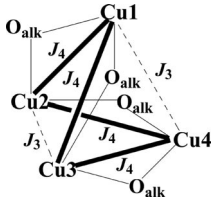

Scheme 2.

In view of this, we decided to simulate the data with the Hamiltonian [Equation (1); here for complex **2**, $J_2 = J_3$ and $J_1 = J_4$] by keeping $J_3 = 0$. The calculated parameters were $J_4 = -154.6\ cm^{-1}$, $g = 2.17$, and $\rho = 0.3\%$ with a fixed TIP value of $240 \times 10^{-6}\ cm^3\,mol^{-1}$. By using the J_4 and J_3 values from DFT calculations (see below) as a starting point for the fit of the experimental data, the following parameters were obtained: $J_4 = -155.1\ cm^{-1}$, $J_3 = -1.0\ cm^{-1}$, $g = 2.174$, and $\rho = 0.3\%$ with a fixed TIP of $240 \times 10^{-6}\ cm^3\,mol^{-1}$ ($R = 2 \times 10^{-4}$).

In complex **1**, the two copper centers are linked equatorially by a bridging alkoxido group; they are also bridged by a cresolato group coordinated axially, whereas in **2** the copper ions are connected by an alkoxido group. It has also been stated that when the copper centers are connected axially by a bridging phenoxido group, they exhibit very weak ferro- and antiferromagnetic or no interaction.[26–28] Thus, in our case, the magnetic exchange is mediated principally

through alkoxido bridges. Both theoretical and experimental studies have shown that the major factor controlling the magnetic exchange interaction in dialkoxido-bridged dicopper(II) complexes is the value of the Cu–O–Cu angle and a linear variation of J with θ (the Cu–O–Cu angle).[30] DFT calculations carried out on alkoxido-bridged model compounds[30–32] that contain a planar $Cu_2(\mu\text{-}O_2)$ skeleton and a methyl group bonded to each oxygen atom of the double bridge predicted antiferromagnetic interactions for the whole range of Cu–O–Cu (θ) when τ values (out-of-plane displacement of the carbon atom from the Cu_2O_2 plane) were smaller than 40°. The antiferromagnetic (AF) coupling is favored when θ increases and τ diminishes. Therefore, in complexes **1** and **2** with very large $Cu–O_{alkoxido}–Cu$ angles (θ = 130.11° for **1** and θ_{av} = 123° for **2**) strong antiferromagnetic interactions are expected. However, antiferromagnetic interaction with moderate J values (J_1 = –104.2 cm^{-1} for **1** and J_4 = –155.1 cm^{-1} for **2**) are observed. We attribute this behavior mainly to: (i) the existence of only one alkoxido bridging group between each pair of copper(II) atoms, and (ii) the out-of-plane displacement of the alkoxido carbon atom from the Cu–O–Cu plane (τ). In **1**, the τ angle is rather high (30.28°), and therefore a significant decrease of the antiferromagnetic interaction with respect to that predicted by the θ angle (130.11°) is expected. In the case of **2**, the average τ angle is 9.5°, and consequently a stronger antiferromagnetic interaction is observed for this compound.

Computational Details

The density functional method has been employed to study the magnetic coupling in the complexes. X-ray coordinates of the cationic part of the complex have been used to calculate the exchange coupling constant, as small changes in the coordination environment can strongly influence its magnetic properties. We have replaced the methyl group by a hydrogen atom in **1** and the $–CH_2–CH(CH_3)_2$ group by a $–CH_3$ group in the ligand framework of **2** to reduce the considerable amount of computational work. To explain the exchange coupling constant for polynuclear complexes, the spin Hamiltonian $\hat{H} = -J\hat{S}_i\hat{S}_j$ is used, in which $\hat{S}_i$ and $\hat{S}_j$ stand for the different paramagnetic centers.

In the present tetranuclear complexes, the two J values (J_1 and J_2 for **1** and J_3 and J_4 for **2**) have been obtained by calculating the corresponding energy of three different states. For both the complexes there are eight independent spin configurations (considering only the up-spin) that have one quintet state (QS), four equivalent triplet states (TS), and three broken-symmetry states (BS) out of which two are equivalent (BS1) and one is different (BS2). The different energy states for complex **1** and **2** are given in Schemes 3 and 4, respectively.

Equations (2), (3), (4), (5), (6) and (7) were obtained from the different energy states.

$$E_{QS} - E_{BS1} = -4J_1 \quad (2)$$

$$E_{QS} - E_{BS2} = -(2J_1 + 2J_2) \quad (3)$$

$$E_{QS} - E_{TS} = -(J_2 + 2J_1) \quad (4)$$

$$E_{QS} - E_{BS1} = -4J_4 \quad (5)$$

$$E_{QS} - E_{BS2} = -(2J_3 + 2J_4) \quad (6)$$

$$E_{QS} - E_{TS} = -(J_3 + 2J_4) \quad (7)$$

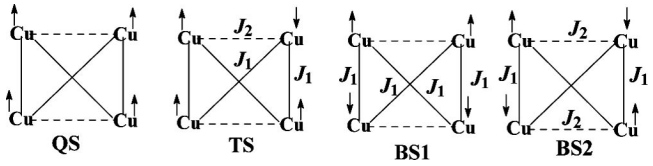

Scheme 3. Different energy states for complex **1**.

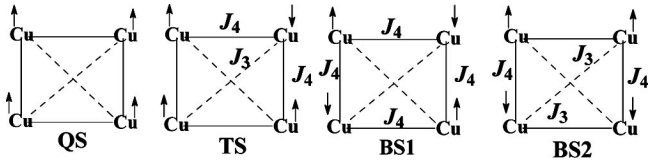

Scheme 4. Different energy states for complex **2**.

Equations (2), (4), (5), and (7) have been employed to calculate the exchange coupling constants, whereas Equations (3) and (6) have not been taken into account due to no or negligible contribution of J_2 and J_3 for **1** and **2**, respectively.

The terms E_{QS}, E_{TS}, and E_{BS} correspond to the energy of quintet, triplet, and broken-symmetry states, respectively; J_1 and J_2 denote, respectively, the coupling constants for the two copper centers bridged by an alkoxido and phenoxido group in **1** (Scheme 1), whereas for **2**, J_3 and J_4 represent the exchange interaction between the two nearest copper centers bridged by an alkoxido group and unassociated next-nearest copper centers, respectively (Scheme 2). The positive and the negative value of the coupling constant J indicates the ferromagnetic and antiferromagnetic ground states of the system, respectively.

Magnetic Exchange Interaction and DFT Study

The spin densities of the high-spin state for the two complexes were calculated to understand the electronic structure and hence their magnetic behavior. The delocalization of the spin density of the unpaired electron between the paramagnetic centers through the suitable orbital of the bridging ligand is responsible for the antiferromagnetic interaction. The participation of the coordinating atoms of the ligand in the formation of the singly occupied molecular orbital (SOMO) leads to the enhancement of the degree of delocalization of the unpaired electrons, which increase the antiferromagnetism of the molecule. The calculated spin densities that correspond to the high-spin state for the two complexes are given in Table 3, and the calculated J values are given in Table 4.

Table 3. Calculated Mulliken spin densities for complexes **1** and **2**.

Complex	Cu	μ-$O_{phenoxido}$	μ-$O_{alkoxido}$	N_{av}
1	0.6335	0.0042	0.1663	0.1040
2	0.5944	–	0.1509	0.1361

Table 4. Calculated exchange coupling constants J [cm^{-1}] of real molecules and model systems.

J [cm^{-1}]	Complexes/models					
	1	**2**	**3**	**4**	**5**	**6**
J_1	–82.3	–	–76	–	–	–
J_2	–2.5	–	–	–2.1	–	–
J_3	–	–1.6	–	–	–0.2	–
J_4	–	–127	–	–	–	–114

It is clear from the spin density plots (Figures 5 and 6) that in both cases the spin density is mainly distributed between the $d_{x^2-y^2}$ orbital of copper atoms and the hybrid orbitals of the donor atoms in the equatorial plane.

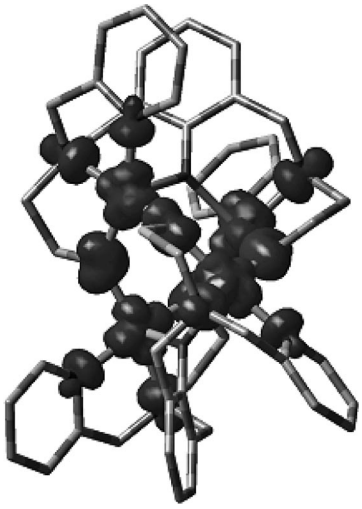

Figure 5. Spin density plot that corresponds to the high-spin state for **1** (isosurface cutoff value = 0.004).

Thus, here the magnetic exchange coupling is propagated mainly through the $d_{x^2-y^2}$ orbital of the copper(II) ion with the appropriate hybrid orbitals of the alkoxido oxygen atoms. The calculated spin density of the cresolato group accounts for no or negligible exchange interaction through the cresolato group in **1**. Therefore, it is believed that the exchange interaction between the copper atoms bridged through the cresolato group in **1** and the next-nearest neighboring copper atoms (having no direct connectivity) in **2** are taking place by through-space overlap between the magnetic orbitals of the metal ions.

We have also analyzed the individual exchange coupling constants (J_1, J_2, J_3, and J_4) in an alternative way in which two Cu^{II} ions are replaced by two Zn^{II} ions. The replacement with Zn^{II} ions produced a Cu_2Zn_2 complex that became magnetically equivalent to a dinuclear copper(II) complex.[33,34] By using this model, we have calculated the

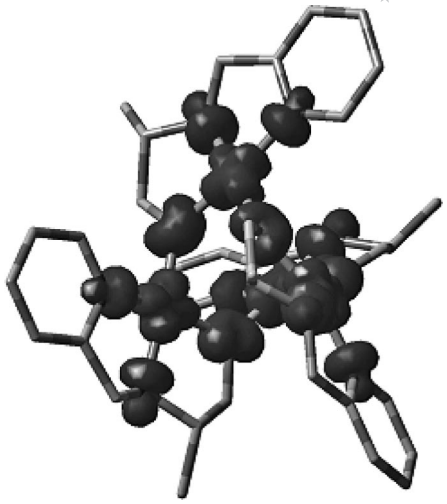

Figure 6. Spin density plot that corresponds to the high-spin state for **2** (isosurface cutoff value = 0.004).

different J values depending on which copper atoms are replaced by zinc atoms. The schematic diagram is depicted in Scheme 5 (parts 3, 4, 5, and 6).

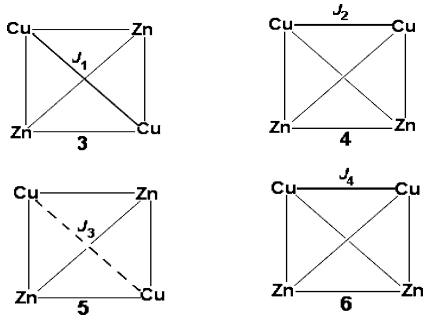

Scheme 5.

The individual J values (Table 4) calculated from the Cu_2Zn_2 model systems are well matched with the J values of the real molecule. In summary, the DFT study is in agreement with the experimental results.

Conclusion

In the present article we have presented the synthesis, structure, and magnetic studies of tetranuclear complexes $[Cu_4(L^1)_2](ClO_4)_2$ (**1**) and $[Cu_4(L^2)_4](ClO_4)_4$ (**2**) with symmetrical N_4O_3 coordinating heptadentate and N_2O coordinating ligands, respectively. Complex **1** bears a Cu_4O_6 core, whereas **2** contains a Cu_4O_4 core. In both cases, an overall antiferromagnetic interaction is observed as a result of dominant antiferromagnetic interactions through alkoxido bridges. In compounds **1** and **2** the predominant magnetic core is [Cu–(μ-$O_{alkoxido}$)–Cu] (θ = 123–130°), but the relatively small $|J|$ values in the 100–154 cm^{-1} range can be explained by the existence of only one alkoxido group bridging each pair of copper(II) atoms and the out-of-plane displacement of the alkoxido carbon atom from the Cu–O–Cu plane. The magnetic exchange pathway for both cases has

been examined with the help of BSDFT calculation. A search for new polynuclear copper(II) complexes with different polydentate ligands is in progress.

Experimental Section

Materials: All the starting chemicals were analytically pure and used without further purification. The ligand was prepared similarly according to a literature procedure.[35,36] ***Caution:*** Perchlorate salts are highly explosive, and should be handled with care and in small amounts!

Physical Measurements: UV/Vis and IR spectra were recorded with a Perkin–Elmer LAMBDA EZ-301 spectrophotometer and a Perkin–Elmer 1-0100 spectrometer, respectively. Electrochemical measurements (samples in acetonitrile) were performed with a CHI 620A electrochemical analyzer using a platinum electrode. Tetraethylammonium perchlorate (TEAP) was used as a supporting electrolyte, and the potentials were referenced to the SCE without junction correction. Elemental analysis (C, H, N) was performed with a Perkin–Elmer 2400 Series II elemental analyzer. Electron paramagnetic resonance (EPR) experiments were performed with a Varian E-109C (X-band, 9.1 GHz) spectrometer at a microwave power of 30 dB and modulation amplitude of 12.5 G, and spectra were collected by using a quartz dewar for measurements at liquid-nitrogen temperature. Diphenylpicrylhydrazyl (dpph, g = 2.0037) was used to calibrate the spectra. Magnetic measurements were carried out on polycrystalline samples with a Quantum Design MPMS XL SQUID susceptometer operating at a magnetic field of 0.5 T from room temperature to 2 K and at 0.03 T from 2 to 50 K. The results for both fields were coincident. The diamagnetic corrections were evaluated from Pascal's constants.

Crystallographic Studies: Single crystals of suitable quality for single-crystal X-ray diffraction studies were grown by slow concentration of solutions of complexes **1** and **2** in acetonitrile. The X-ray intensity data were measured at 293 K with a Bruker Nonius SMART APEX CCD diffractometer (Mo-K_α, λ = 0.71073 Å). The detector was placed at a distance of 6.0 cm from the crystal. A total of 606 frames were collected with a scan width of 0.3° in different settings of ϕ. The data were reduced using SAINTPLUS,[37] and the empirical absorption correction was applied using the SADABS package.[38] Metal atoms were located by direct methods, and the rest of the non-hydrogen atoms emerged from successive Fourier synthesis. The structure was refined by full-matrix least-squares procedures on F^2. The perchlorate oxygen atoms for **1** (O3, O4, O5) and **2** (O7, O8, O13, O14, O17, O18) were refined isotropically, and all the remaining non-hydrogen atoms for both cases were refined anisotropically. All the hydrogen atoms were included in calculated positions. Calculations were performed using version 6.14 of the SHELXTL[39] program package. Molecular structure plots were drawn using ORTEP.[40] Relevant crystal data are given in Table 5. CCDC-724535 (**1**) and -724535 (**2**) contain the supplementary crystallographic data for this paper. These data can be obtained free of charge from The Cambridge Crystallographic Data Centre via www.ccdc.cam.ac.uk/data_request/cif.

Table 5. Crystal data and structure-refinement parameters for complexes **1** and **2**.

	1	**2**
Empirical formula	$C_{58}H_{74}Cl_{2.67}Cu_4N_8O_{18}$	$C_{48}H_{76}Cl_4Cu_4N_8O_{19.5}$
M_r	1519.95	1473.13
Crystal system	cubic	tetragonal
Space group	$Fd\bar{3}c$	$P4_12_12$
a [Å]	43.124(5)	17.113(4)
b [Å]	43.124(5)	17.113(4)
c [Å]	43.124(5)	44.150(4)
V [Å^3]	80199(16)	12930(4)
Z	48	8
$\rho_{calcd.}$ [mg m^{-3}]	1.511	1.514
μ [mm^{-1}]	1.435	1.536
θ [°]	1.64–26.09	1.28–21.63
T [K]	293(2)	293(2)
$R1$,[a] $wR2$[b] [$I > 2\sigma(I)$]	0.0594, 0.1929	0.0603, 0.1632
GOF on F^2	1.086	1.051

[a] $R1 = \Sigma||F_o| - |F_c||/\Sigma|F_o|$. [b] $wR2 = [\Sigma w(F_o^2 - F_c^2)^2/\Sigma w(F_o^2)^2]^{1/2}$.

DFT Calculations: The magnetic exchange interaction between the transition-metal ions was studied on the basis of density functional theory coupled with the broken-symmetry approach[41] for weakly interacting magnetic ions. It has been cited in the literature that exchange coupling constants J are often overestimated in DFT calculations.[42] Despite that, the broken-symmetry solution is very useful in understanding the exchange pathways for polynuclear transition-metal complexes.[37] Thus, in the present case, we have performed the DFT calculations with broken symmetry for monitoring the exchange pathways involved in the system. Ground-state electronic-structure calculations of the complexes have been carried out using density functional theory (DFT)[43] methods with the Gaussian 03 program.[44] Becke's hybrid function[45] with the Lee–Yang–Parr (LYP) correlation function[46] was used through the study. We used the 6-31G basis set for H atoms, a double-ζ all-electron basis set[47] for C, N, O atoms, and LANL2DZ valance and an effective core potential was applied for the copper atoms. All energy calculations were performed using the SCF = Tight option of the Gaussian program to ensure sufficiently well-converged values for the state energies.

Synthesis of Complexes

$[Cu_4(L^1)_2](ClO_4)_2$ (1): Ligand H_3L^1 (0.246 g, 0.5 mmol) was added to a solution of copper(II) perchlorate hexahydrate (0.372 g, 1.0 mmol) in methanol (30 mL), and the resulting solution was stirred at room temperature for 0.5 h, followed by addition of triethylamine. During stirring, a green precipitate separated from the solution. The green residue was separated by filtration and recrystallized from acetonitrile to yield a green crystalline product. Yield: 0.250 g (70%). $C_{58}H_{74}Cl_2Cu_4N_8O_{14}$ (1432.36): calcd. C 48.63, H 5.21, N 7.82; found C 49.21, H 5.15, N 7.75. UV/Vis (CH_3CN): λ_{max} (ε) = 251 (27277), 317 (11682), 755 (467 M^{-1} cm^{-1}) nm. IR (KBr): $\nu(ClO_4^-)$ = 1091, 623 cm^{-1}; $\nu(CO_{phenoxido})$ = 1337 cm^{-1}; $\nu(CO_{alkoxido})$ = 1051 cm^{-1}. $E_{pa}(Cu^{II}/Cu^{III})$ = 0.95 V (irr.); $E_{pc}(Cu^{II}/Cu^{I})$ = –0.76 V (irr.).

$[Cu_4(L^2)_4](ClO_4)_4$ (2): HL^2 (0.208 g, 1.0 mmol) was added to a solution of copper(II) perchlorate hexahydrate (0.372 g, 1.0 mmol) in methanol (25 mL). The mixture was stirred at room temperature for 1.0 h, and then triethylamine was added. Upon stirring, a blue precipitate formed. The blue precipitate was filtered and recrystallized from acetonitrile to yield a blue crystalline product. Yield: 0.267 g (72%). $C_{48}H_{76}Cl_4Cu_4N_8O_{20}$ (1481.17): calcd. C 38.92, H 5.17, N 7.57; found C 38.41, H 5.12, N 7.48. UV/Vis (CH_3CN): λ_{max} (ε) = 255 (32775), 283 (12980), 656 (502 M^{-1} cm^{-1}) nm. IR (KBr): $\nu(ClO_4^-)$ = 1093, 625 cm^{-1}; $\nu(CO_{alkoxido})$ = 1024 cm^{-1}. $E_{pa}(Cu^{II}/Cu^{III})$ = 1.35 V (irr.); $E_{pc}(Cu^{II}/Cu^{I})$ = –0.82 V (irr.).

Acknowledgments

Financial support from the Department of Science and Technology, New Delhi, India, the Council of Scientific and Industrial Re-

search, New Delhi, India, and the University Grant Commission, New Delhi is gratefully acknowledged. We are thankful to DST for the data collection on the National Single Crystal X-ray Diffractometer Facility setup at the School of Chemistry, University of Hyderabad, Hyderabad, India, and the Indian Association for the Cultivation of Science (IACS), Jadavpur, India. E. C. thanks the Ministerio de Educación y Ciencia (MEC), Spain (Projects CTQ2005/0935 and CTQ-2008-02269/BQU) and the Junta de Andalucía (FQM-195) for financial support.

[1] *Handbook of Metalloproteins*, vol. 2 (Eds.: A. Messerschmidt, R. Huber, T. Poulos, K. Wieghardt), Wiley, New York, **2001**.
[2] R. H. Holm, P. Kennepohl, E. I. Solomon, *Chem. Rev.* **1996**, *96*, 2239–2314.
[3] *Magnetism: Molecules to Materials* (Eds.: J. S. Miller, M. Drillon), Wiley-VCH, Weinheim, Germany, **2002**.
[4] Preface: K. R. Dunbar, "Special Issue on New Horizons for Magnetic Solids Based on Molecules: From High-T_c Magnets to Nanomagnets to Devices" in *J. Solid State Chem.* **2001**, *159*, 251–252.
[5] O. Kahn, *Molecular Magnetism*, Wiley-VCH, New York, **1993**.
[6] *Research Frontiers in Magnetochemistry* (Ed.: C. J. O'Connor), World Scientific, Singapore, **1993**.
[7] *Magnetic Molecular Materials* (Eds.: D. Gatteschi, O. Kahn, J. S. Miller, F. Palacio), Kluwer Academic Publishers, Dordrecht, The Netherlands, **1991**.
[8] A. J. Tasiopoulos, S. P. Perlepes, *Dalton Trans.* **2008**, 5537–5555.
[9] O. Waldmann, A. M. Ako, H. U. Gudel, A. K. Powell, *Inorg. Chem.* **2008**, *47*, 3486–3488.
[10] D. Gatteschi, R. Sessoli, *Angew. Chem. Int. Ed.* **2003**, *42*, 268–297.
[11] R. Sessoli, D. Gatteschi, A. Caneschi, A. M. Novak, *Nature* **1993**, *365*, 141–143.
[12] A. Burkhardt, E. T. Spielberg, H. Görls, W. Plass, *Inorg. Chem.* **2008**, *47*, 2485–2493.
[13] S. Roy, T. N. Mandal, A. K. Barik, S. Pal, R. J. Butcher, M. Salah EI Fallah, J. Tercero, S. K. Kar, *Dalton Trans.* **2007**, 1229–1234.
[14] J. Tercero, E. Ruiz, S. Alvarez, A. Rodriguez-Fortea, P. Alemany, *J. Mater. Chem.* **2006**, *16*, 2729–2735.
[15] M. Salah EI Fallah, F. Badyine, R. Vicente, A. Escuer, X. Solans, M. Font-Bardia, *Dalton Trans.* **2006**, 2934–2942.
[16] Z. Xu, L. K. Thompson, D. O. Miller, *J. Chem. Soc., Dalton Trans.* **2002**, 2462–2466.
[17] A. Kavlakoglu, A. Elmali, Y. Elerman, I. Svoboda, *Polyhedron* **2002**, *21*, 1539–1545.
[18] E. Ruiz, A. Rodriguez-Fortea, P. Alemany, S. Alvarez, *Polyhedron* **2001**, *20*, 1323–1327.
[19] L. K. Thompson, C. J. Matthews, L. Zaho, Z. Xu, D. O. Miller, C. Wilson, M. A. Leech, J. A. K. Howard, S. L. Heath, A. G. Whittaker, E. P. Winpenny, *J. Solid State Chem.* **2001**, *159*, 308–320.
[20] C. J. Matthews, K. Avery, Z. Xu, L. K. Thompson, L. Zaho, D. O. Miller, K. Biradha, K. Poirier, M. J. Zaworotko, C. Wilson, A. E. Goeta, J. A. K. Howard, *Inorg. Chem.* **1999**, *38*, 5266–5276.
[21] K. Nakamoto, *Infrared and Raman Spectra of Inorganic and Coordination Compounds*, 4th ed., Wiley, New York, **1986**, pp. 191.
[22] B. P. Murch, F. C. Bradley, P. D. Boyle, V. Papafthymiou, L. Que Jr., *J. Am. Chem. Soc.* **1987**, *109*, 7993–8003.
[23] E. I. Solomon, M. J. Bladwin, M. D. Lowery, *Chem. Rev.* **1992**, *92*, 521–542.
[24] a) G. A. van Albada, M. T. Lakin, N. Veldman, A. L. Spek, J. Reedijk, *Inorg. Chem.* **1995**, *34*, 4910–4917; b) G. A. van Albada, W. J. J. Smeets, A. L. Spek, J. Reedijk, *Inorg. Chim. Acta* **1997**, *260*, 151–161.
[25] C. O'Sullivan, G. Murphy, B. Murphy, B. Hathaway, *J. Chem. Soc., Dalton Trans.* **1999**, 1835–1844.
[26] J. Manzur, H. Mora, A. Vega, E. Spodine, D. V. Yazigi, M. T. Garland, M. Salah EI Fallah, A. Escuer, *Inorg. Chem.* **2007**, *46*, 6924–6932.
[27] H. P. Berends, D. W. Stephan, *Inorg. Chem.* **1987**, *26*, 749–754.
[28] A. Mukherjee, M. K. Saha, I. Rudra, S. Ramasesha, M. Nethaji, A. R. Ckakravarty, *Inorg. Chim. Acta* **2004**, *357*, 1077–1082.
[29] a) J. J. Borrás-Almenar, J. Clemente, E. Coronado, B. S. Tsukerblat, *Inorg. Chem.* **1999**, *38*, 6081–6088; b) J. J. Borrás-Almenar, J. Clemente, E. Coronado, B. S. Tsukerblat, *J. Comput. Chem.* **2001**, *22*, 985–991.
[30] a) L. Merz, W. Haase, *J. Chem. Soc., Dalton Trans.* **1980**, 875; b) M. Handa, N. Koga, S. Kida, *Bull. Chem. Soc. Jpn.* **1988**, *61*, 3853–3857.
[31] L. K. Thompson, S. K. Mandal, S. S. Tandon, J. N. Bridson, M. K. Park, *Inorg. Chem.* **1996**, *35*, 3117–3125.
[32] a) H. Astheimer, W. Haase, *J. Chem. Phys.* **1986**, *85*, 1427–1432; b) E. Ruiz, P. Alemany, S. Alvarez, J. Cano, *J. Am. Chem. Soc.* **1997**, *119*, 1297–1303; c) E. Ruiz, P. Alemany, S. Alvarez, J. Cano, *Inorg. Chem.* **1997**, *36*, 3683–3688; d) H. Hu, D. Zhang, Z. Chen, C. Liu, *Chem. Phys. Lett.* **2000**, *329*, 255–260; e) H. Hu, X. Yang, Z. Chen, *THEOCHEM* **2002**, *618*, 41–46; f) H. Hu, Y. Liu, D. Zhang, C. Liu, *THEOCHEM* **2001**, *546*, 73–78; g) L. J. Farrugia, D. S. Middlemiss, R. Sillanpää, P. Seppälä, *J. Phys. Chem. Part A* **2008**, *112*, 9050–9067.
[33] E. Ruiz, A. Rodriguez-Fortea, J. Cano, S. Alvarez, P. Alemany, *J. Comput. Chem.* **2003**, *24*, 982–989.
[34] A. Bencini, F. Totti, *J. Chem. Theory Comput.* **2009**, *5*, 144–154.
[35] A. Mondal, S. Sarkar, D. Chopra, T. N. Guru Row, K. Pramanik, K. K. Rajak, *Inorg. Chem.* **2005**, *44*, 703–708.
[36] S. Larsen, K. Michelsen, E. Pedersen, *Acta Chem. Scand.* **1986**, *A40*, 63–76.
[37] a) L. Noodleman, J. G. Morman Jr., *J. Chem. Phys.* **1979**, *70*, 4903–4906; b) J. E. Mc Grady, R. Stranger, *J. Am. Chem. Soc.* **1997**, *119*, 8512–8522.
[38] *SMART, SAINT, SADABS, XPREP, SHELXTL*, Bruker AXS Inc., Madison, WI, **1998**.
[39] G. M. Sheldrick, *SHELXTL*, version 6.14, Bruker AXS Inc., Madison, WI, **2003**.
[40] C. K. Johnson, ORTEP, Report ORNL-5138, Oak Ridge National Laboratory, Oak Ridge, TN, **1976**.
[41] a) L. Noodleman, D. A. Case, *Adv. Inorg. Chem.* **1992**, *38*, 423–470; b) L. Noodleman, E. J. Baerends, *J. Am. Chem. Soc.* **1984**, *106*, 2316–2327; c) L. Noodleman, *J. Chem. Phys.* **1981**, *74*, 5737–5743.
[42] a) X. G. Zhao, W. H. Richardson, J. L. Chen, L. Noodleman, H. L. Tasi, D. N. Hendrickson, *Inorg. Chem.* **1997**, *36*, 1198–1217; b) A. Bencini, F. Totti, C. A. Daul, K. Doclo, P. Fantucci, V. Barone, *Inorg. Chem.* **1997**, *36*, 5022–5030; c) C. Adamo, V. Barone, A. Bencini, F. Totti, I. Ciofini, *Inorg. Chem.* **1999**, *38*, 1996–2004; d) T. Soda, Y. Kitagawa, T. Onishi, Y. Yakano, Y. Shigeta, H. Nagao, Y. Yoshioka, K. Yamaguchi, *Chem. Phys. Lett.* **2000**, *319*, 223–230; e) M. J. Prushan, D. M. Tomezsko, S. Lofland, M. Zeller, A. D. Hunter, *Inorg. Chim. Acta* **2007**, *360*, 2245–2254.
[43] R. G. Parr, W. Yang, *Density Functional Theory of Atoms and Molecules*, Oxford University Press, Oxford, **1989**.
[44] M. J. Frisch, G. W. Trucks, H. B. Schlegel, G. E. Scuseria, M. A. Robb, J. R. Cheeseman, J. A. Montgomery Jr., T. Vreven, K. N. Kudin, J. C. Burant, J. M. Millam, S. S. Iyengar, J. Tomasi, V. Barone, B. Mennucci, M. Cossi, G. Scalmani, N. Rega, G. A. Petersson, H. Nakatsuji, M. Hada, M. Ehara, K. Toyota, R. Fukuda, J. Hasegawa, M. Ishida, T. Nakajima, Y. Honda, O. Kitao, H. Nakai, M. Klene, X. Li, J. E. Knox, H. P. Hratchian, J. B. Cross, V. Bakken, C. Adamo, J. Jaramillo, R. Gomperts, R. E. Stratmann, O. Yazyev, A. J. Austin, R. Cammi, C. Pomelli, J. W. Ochterski, P. Y. Ayala, K. Morok-

uma, G. A. Voth, P. Salvador, J. J. Dannenberg, V. G. Zakrzewski, S. Dapprich, A. D. Daniels, M. C. Strain, O. Farkas, D. K. Malick, A. D. Rabuck, K. Raghavachari, J. B. Foresman, J. V. Ortiz, Q. Cui, A. G. Baboul, S. Clifford, J. Cioslowski, B. B. Stefanov, G. Liu, A. Liashenko, P. Piskorz, I. Komaromi, R. L. Martin, D. J. Fox, T. Keith, M. A. Al-Laham, C. Y. Peng, A. Nanayakkara, M. Challacombe, P. M. W. Gill, B. Johnson, W. Chen, M. W. Wong, C. Gonzalez, J. A. Pople, *Gaussian 03*, Revision C.02, Gaussian, Inc., Wallingford, CT, **2004**.

[45] A. D. Becke, *J. Chem. Phys.* **1993**, *98*, 5648–5652.

[46] C. Lee, W. Yang, R. G. Parr, *Phys. Rev. B* **1998**, *37*, 785–789.

[47] A. Schaefer, H. Horn, R. Ahlrichs, *J. Chem. Phys.* **1992**, *97*, 2571–2577.

Received: July 24, 2009
Published Online: January 5, 2010

